ELSEVIER

Volumes 301–302 April 2007 ISSN 0022-0248

JOURNAL OF CRYSTAL GROWTH

14th International Conference on Molecular Beam Epitaxy (MBE-XIV)

3 – 8 September 2006
Waseda University,
Tokyo, Japan

Guest Editors:
J. Yoshino
H. Akinaga
H. Asahi

Available online at www.sciencedirect.com
ScienceDirect
Journal of Crystal Growth 301–302 (2007) 525–528
JOURNAL OF CRYSTAL GROWTH
www.elsevier.com/locate/jcrysgro

All-GaInNAs ultrafast lasers: Material development for emitters and absorbers

A. Rutz[a,*], V. Liverini[a], E. Müller[b], S. Schön[c], U. Keller[a]

[a]*ETH Zurich, Physics Department, Institute of Quantum Electronics, Wolfgang-Pauli-Strasse 16, CH-8093 Zürich, Switzerland*
[b]*ETH Zurich, Physics Department, Laboratory for Solid State Physics, Wolfgang-Pauli-Strasse 16, CH-8093 Zürich, Switzerland*
[c]*ETH Zurich, FIRST Center for Micro- and Nanoscience, Wolfgang-Pauli-Strasse 10, CH-8093 Zürich, Switzerland*

Available online 5 February 2007

Abstract

Defect engineering is a key feature in material development for active and passive laser devices. Active devices such as surface emitting lasers require excellent material quality with low defect concentration and good strain management. In contrast, passive devices such as saturable absorbers benefit from nonradiative recombination via defect states. Different molecular beam epitaxy (MBE) growth conditions and annealing parameters were developed to optimize GaInNAs for both active and passive devices. We have demonstrated for the first time an all-GaInNAs modelocked vertical external-cavity surface-emitting laser (VECSEL) at 1.3 μm. We combined a GaInNAs VECSEL with a GaInNAs semiconductor saturable absorber mirror (SESAM) in a laser cavity. The VECSEL was optically pumped by an 808 nm semiconductor diode laser. The intracavity GaInNAs SESAM self-starts stable modelocking and generates a pulse duration of 18.7 ps with a pulse repetition rate of 6.1 GHz at 57 mW of average output power at a center wavelength of 1308 nm. In this paper, we briefly review the modelocking result and then focus on the MBE growth and fabrication of both active and passive GaInNAs devices.

PACS: 71.55.Eq; 78.45.+h; 42.55.Px; 42.65.Re; 42.60.Fc

Keywords: A3. Molecular beam epitaxy; B1. Nitrides; B2. Semiconducting quaternary alloys

1. Introduction

GaInNAs is a promising gain material for low-cost laser sources at 1.3–1.5 μm wavelength [1,2]. A main advantage of using GaInNAs on GaAs compared to InP-based systems is the availability of high-quality (Al)GaAs/AlAs distributed Bragg reflectors (DBRs) with a reasonable refractive index contrast and good thermal properties. Such mirrors are crucial for high-performance vertical external-cavity surface-emitting lasers (VECSELs) [3]. We have demonstrated that GaInNAs is also very useful as a fast-recovering absorber material when grown under different conditions both for an operation wavelength of 1.3 μm [4,5] and 1.5 μm [6]. Integrating GaInNAs absorber layers into a semiconductor saturable absorber mirror (SESAM) [7–9], we have successfully modelocked diode-pumped solid-state lasers [4,6,10]. In this paper, we report a passively modelocked optically pumped GaInNAs VECSEL [11]. Ultrafast optically pumped VECSELs offer high average output power at near diffraction-limited beam quality [12]. Such lasers are interesting for broadband optical communication, optical clocking of future microprocessors or for laser display projection systems using additional frequency doubling. GaInNAs-based VECSELs were already demonstrated by Hopkins et al. [13], however, modelocking was not obtained before.

The defect concentration in GaInNAs is known to be very sensitive on growth conditions and on the following annealing procedures [14]. For absorber materials, a large number of nonradiative defects is necessary to reduce the recovery time while at the same time, the nonsaturable losses due to absorption or light scattering need to be kept as low as possible. For a laser gain material, however, very

*Corresponding author. Tel.: +41 44 633 40 61; fax: +41 44 633 10 59.
E-mail address: arutz@phys.ethz.ch (A. Rutz).

0022-0248/$ - see front matter © 2007 Published by Elsevier B.V.
doi:10.1016/j.jcrysgro.2006.11.261

low defect concentrations are necessary to achieve high efficiency and a low laser threshold. This is achieved by applying different growth conditions and a suitable post-growth annealing process. In this paper, we discuss the different growth and annealing procedures for the gain medium and the absorber, as well as the laser results obtained using a GaInNAs VECSEL and SESAM.

2. Growth, characterization and annealing instrumentation

The active and passive devices were grown using a Veeco Gen-III solid-source molecular beam epitaxy (MBE) and a Veeco Uni-Bulb RF-plasma source for nitrogen incorporation. The growth temperature was monitored using band-edge thermometry. Post-growth rapid thermal annealing (RTA) experiments as well as in situ annealing under constant As_2 flux were carried out. X-ray rocking curve (XRC) and room temperature photoluminescence (PL) measurements were used to characterize composition, layer thickness and defect concentration. Transmission electron microscopy (TEM) cross-sections were used to check for interface flatness, uniform indium distribution and confirmation of fully pseudomorphic growth.

3. Material growth and device fabrication

Different growth and annealing properties were investigated using single- and multiple quantum well (QW) $Ga_xIn_{1-x}N_yAs_{1-y}$ structures fabricated as VECSELs and SESAMs with a QW thickness d of 8 or 10 nm, and a stoichiometry of $x = 0.65$, and $y = 0.018$ or 0.016.

High-efficiency GaInNAs VECSELs are obtained only with a combination of optimized growth conditions and a suitable post-growth thermal annealing process. We found the best results by applying a growth temperature of 410 °C at a As/III BEP ratio of about 25. As-grown samples exhibit a quite low PL intensity that improves drastically upon thermal annealing. The low growth temperature was chosen to minimize surface mobility on the growth interface to obtain two-dimensional growth and reduced nitrogen-rich cluster formation. However, many point defects are formed due to the low growth temperature. These point defects are removable by post-growth annealing to a certain extent. Defects introduced by nitrogen incorporation at higher temperatures are much more resistant to annealing. The optimum growth temperature is found at the point where these two combined defect-creating effects result in the lowest number of nonradiative recombination channels after annealing. The annealing parameters temperature and time play an important role not only for improving the optical quality of the material but also to control the blueshift of the laser wavelength [15]. It is very important to achieve a saturation of the wavelength blueshift to correctly predict the lasing wavelength of the gain material because its low-temperature growth is followed by a long high-temperature exposure during the subsequent DBR growth.

Fig. 1 compares the PL intensity of two single QW test structures grown under identical conditions. One was annealed in situ under the same constant As_2 flux as it was used for the QW growth in the MBE chamber for 4 h at 600 °C, while the other initially experienced an additional 5 min period at 700 °C followed by 4 h at 600 °C. Fig. 1 clearly shows that the additional 700 °C annealing period results in a higher PL intensity. The stronger annealing effect is also demonstrated by a slightly larger blue shift. Additional experiments indicated that the 5 min in situ annealing at 700 °C was the maximum possible time and temperature at which the structure did not evaporate in an unacceptable way. The following 4 h at 600 °C were used to ensure blue shift saturation and further improvement of the PL intensity.

The GaInNAs VECSEL consisted of four parts grown upside down on the substrate: (i) an etch-stop structure, (ii) an antireflection structure, (iii) an active region, and (iv) two stacked DBRs for the laser wavelength and the pump light. The total thickness of the laser was 10.2 μm. Fig. 2 shows a high angle annular dark field–scanning transmission electron microscopy (HAADF-STEM) cross-section of the complete structure, which exhibits an excellent interface and mirror layer flatness. The upside-down growth sequence was followed by substrate removal for improved thermal management [16]. The etch-stop

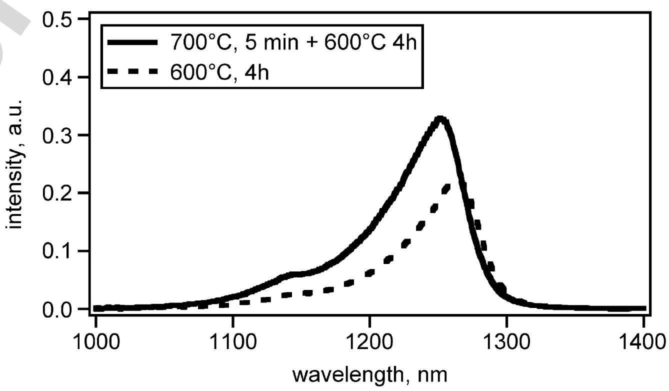

Fig. 1. Relative PL intensities obtained under different annealing conditions for identical sample structures. An additional thermal annealing step at 700 °C was necessary to obtain high optical quality quantum wells and full blueshift saturation.

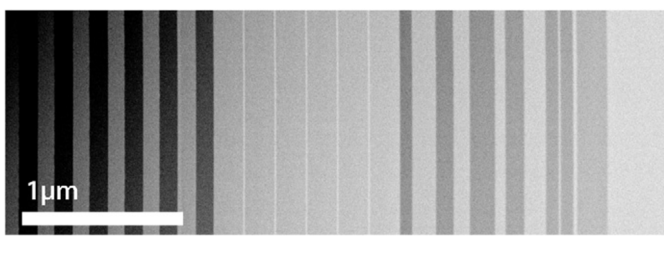

Fig. 2. HAADF-STEM cross-section of a basic GaInNAs VECSEL structure, the DBR is seen on the left, the gain structure containing five 8 nm GaInNAs QWs is visible in the center while the layers on the right side form an antireflection coating and the etch-stop layers.

structure consisted of three sequential layers of $Al_{0.85}Ga_{0.15}As$, GaAs and AlAs for wet-chemical substrate removal. The antireflection structure was made of 10 alternating layers of AlAs and $Al_{0.20}Ga_{0.80}As$ with numerically optimized thicknesses for low reflectivity of both the pump wavelength at 45° of incidence and the laser wavelength at normal incidence. $Al_{0.20}Ga_{0.80}As$ was used in the mirrors instead of pure GaAs, to avoid absorption of the pump wavelength outside of the active region. The active region consisted of five 8-nm-thick $Ga_{0.65}In_{0.35}N_{0.018}As_{0.982}$ QWs separated by 178 nm GaAs barriers to place each QW into the antinodes of the standing wave pattern of the laser electric field as displayed in Fig. 3(a). Finally, the DBRs were grown on top of the structure. The first mirror consisted of a 32-pair $AlAs/Al_{0.20}Ga_{0.80}As$ DBR centered at the laser wavelength of 1300 nm for normal incidence. The second one was a 10-pair DBR of the same materials composition, designed for high reflectivity of the 808 nm pump wavelength at 45° of incidence. After the growth, the structure was metallized by vacuum evaporation of a sequence of Ti, Pt, Au, In and soldered in vacuum to a copper heat sink. The substrate was then removed by lapping and wet chemical etching. This upside-down growth process with subsequent substrate removal was applied to minimize the thermal impedance of the VECSEL to allow for high pump power densities [17].

The GaInNAs SESAM was fully grown by MBE starting with a 35-pair AlAs/GaAs DBR, centered at 1310 nm, on top of which were grown at a 90 nm GaAs spacer layer, a 10 nm $Ga_{0.65}In_{0.35}N_{0.016}As_{0.984}$ absorber, and a 90 nm GaAs cap layer, to make the device antiresonant to obtain negligible group delay dispersion at the central wavelength of 1310 nm [18]. We designed the absorber to be in the antinode of the electric field as shown in Fig. 3(b). The PL emission peak of the GaInNAs absorber corresponds to the onset of the absorption edge and was at 1311 nm. A fast carrier recombination of the absorber was achieved with low-temperature growth at 450 °C without any post-growth annealing. At this relatively high growth temperature, GaInNAs QWs exhibit a slightly three-dimensional growth mode towards the end. It is known for GaInNAs to show carrier localization in QWs, especially when in the as-grown state and grown under nonoptimum conditions. We believe that this localization effect explains the observed low saturation fluence of GaInNAs SESAMs compared to classical materials like InGaAs. The absorber was not annealed after growth to keep the fast nonradiative recombination present in such as-grown QWs. The absorption edge was designed very close to the laser emission wavelength to achieve minimum saturation fluence by keeping the density of states accessible by optical excitation low [5]. This SESAM was characterized by degenerate pump–probe experiments and nonlinear reflectivity measurements [19]. We measured a low saturation fluence of 6.8 ($\pm$0.2) μJ/cm^2, a low modulation depth of 0.76%, non-saturable losses of 0.12% and a recovery time of about 47 ps which is suitable for modelocking with picosecond pulse width [20,21].

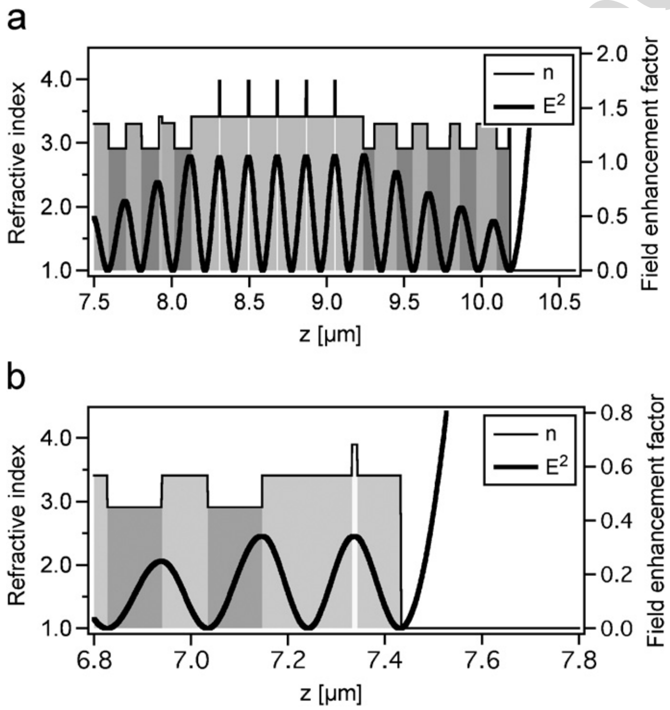

Fig. 3. (a) VECSEL design: refractive index (left axis) and electric field enhancement factor (right axis) as a function of distance in the last 3-µm-thick section of the VECSEL device. (b) SESAM design: refractive index (left axis) and electric field enhancement factor (right axis) in the last 0.6-µm-thick section of the SESAM device.

4. Laser experiments

For laser testing, a simple V-cavity described in detail in Ref. [22] was used. The VECSEL was mounted on a copper heat sink and temperature stabilized by a Peltier element. An 808 nm free-space pump laser diode was positioned at a 45° angle with respect to the VECSEL. Using a 1.5% output coupler, we achieved a cw output power of 200 mW TEM_{00} and 500 mW multimode at 1280 nm with an optical-to-optical slope efficiency of 15.8%. For modelocking, the cavity was rebuilt and a SESAM was inserted. The SESAM was mounted approximately 8 mm away from the VECSEL. A 0.7% transmission output coupler with a radius of curvature of 25 mm was positioned at a distance of about 16 mm from the VECSEL for a total cavity length of 24.7 mm. A 25 µm uncoated fused silica etalon was also placed in the cavity to allow for wavelength stabilization and dispersion management.

We successfully demonstrated for the first time stable self-starting cw modelocking of a GaInNAs VECSEL with a GaInNAs SESAM at 6.1 GHz repetition rate (Fig. 4) [11]. The small peaks at around 20 MHz offset from the main peak at the pulse repetition rate in Fig. 4(b) are suppressed by more than 30 dB. We believe that residual higher-order mode beating is the most likely reason for this instability because they move further away or closer to the

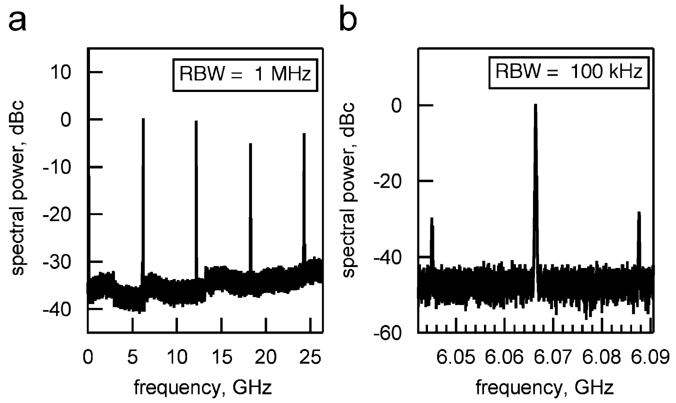

Fig. 4. Microwave spectra: (a) 25 GHz span with a resolution bandwidth of 1 MHz, (b) 50 MHz span with a resolution bandwidth of 100 kHz.

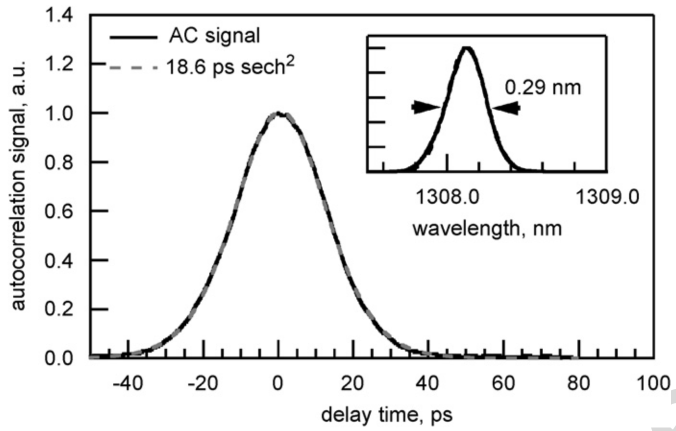

Fig. 5. Intensity autocorrelation: measurement (black solid line) and sech^2 fit (grey dashed line). Inset: optical spectrum with a 0.1 nm resolution.

main peak depending on slight cavity length changes. A pulse duration of 18.7 ps was measured by autocorrelation as shown in Fig. 5. The inset in this figure shows the measured optical spectrum with a FWHM of 0.29 nm obtained with a 0.1 nm resolution optical spectrum analyzer. The average output power was 57 mW, operating the laser with 3 W of pump power and cooling the VECSEL to a temperature of 5 °C.

5. Summary

We have demonstrated the first passively modelocked 1.3 μm VECSEL generating picosecond laser pulses at gigahertz repetition rates. Both the active and the absorbing media are GaInNAs-based QWs, which have optimized growth and annealing parameters for their different applications. A high-temperature annealing step was applied to obtain high optical and crystalline quality for the active GaInNAs QWs.

Acknowledgments

We would like to thank E. Gini and M. Golling for their support with the epitaxy and D. J. H. C. Maas, B. Rudin and A.-R. Bellancourt for their support in the VECSEL design, post-growth processing and modelocking. We received financial support from ETH Zurich and the NCCR-QP program of the Swiss National Science Foundation.

References

[1] H. Riechert, A. Ramakrishnan, G. Steinle, Semicond. Sci. Technol. 17 (2002) 892.
[2] J.J.S. Harris, Semicond. Sci. Technol. 17 (2002) 880.
[3] F. Kuznetsov, F. Hakimi, R. Sprague, A. Mooradian, IEEE J. Selected Top. Quantum Electron. 5 (1999) 561.
[4] V. Liverini, S. Schön, R. Grange, M. Haiml, S.C. Zeller, U. Keller, Appl. Phys. Lett. 84 (2004) 4002.
[5] R. Grange, A. Rutz, V. Liverini, M. Haiml, S. Schön, U. Keller, Appl. Phys. Lett. 87 (2005) 132103.
[6] A. Rutz, R. Grange, V. Liverini, M. Haiml, S. Schön, U. Keller, Electron. Lett. 41 (2005) 321.
[7] U. Keller, K.J. Weingarten, F.X. Kärtner, D. Kopf, B. Braun, I.D. Jung, R. Fluck, C. Hönninger, N. Matuschek, J. Aus der Au, IEEE J. Selected Top. Quantum Electron. 2 (1996) 435.
[8] U. Keller, Nature 424 (2003) 831.
[9] U. Keller, D.A.B. Miller, G.D. Boyd, T.H. Chiu, J.F. Ferguson, M.T. Asom, Opt. Lett. 17 (1992) 505.
[10] G.J. Spuhler, L. Krainer, V. Liverini, R. Grange, M. Haiml, S. Pawlik, B. Schmidt, S. Schon, U. Keller, IEEE Phot. Technol. Lett. 17 (2005) 1319.
[11] A. Rutz, V. Liverini, D.J.H.C. Maas, B. Rudin, A.-R. Bellancourt, S. Schön, U. Keller, Electron. Lett. 42 (2006) 926.
[12] U. Keller, A.C. Tropper, Phys. Rep. 429 (2006) 67.
[13] J.M. Hopkins, S.A. Smith, C.W. Jeon, H.D. Sun, D. Burns, S. Calvez, M.D. Dawson, T. Jouhti, M. Pessa, Electron. Lett. 40 (2004) 30.
[14] M. Kondow, T. Kitatani, S. Shirakata, J. Phys.: Condens. Matter 16 (2004) S3229.
[15] V. Liverini, A. Rutz, U. Keller, S. Schon, J. Appl. Phys. 99 (2006) 113103.
[16] R. Häring, R. Paschotta, A. Aschwanden, E. Gini, F. Morier-Genoud, U. Keller, IEEE J. Quantum Electron. 38 (2002) 1268.
[17] R. Häring, R. Paschotta, E. Gini, F. Morier-Genoud, H. Melchior, D. Martin, U. Keller, Electron. Lett. 37 (2001) 766.
[18] G.J. Spühler, K.J. Weingarten, R. Grange, L. Krainer, M. Haiml, V. Liverini, M. Golling, S. Schon, U. Keller, Appl. Phys. B 81 (2005) 27.
[19] M. Haiml, R. Grange, U. Keller, Appl. Phys. B 79 (2004) 331.
[20] R. Paschotta, R. Häring, U. Keller, A. Garnache, S. Hoogland, A.C. Tropper, Appl. Phys. B 75 (2002) 445.
[21] R. Paschotta, U. Keller, Appl. Phys. B 73 (2001) 653.
[22] A. Aschwanden, D. Lorenser, H.J. Unold, R. Paschotta, E. Gini, U. Keller, Appl. Phys. Lett. 86 (2005) 131102.